

# Zero-field Kondo splitting and quantum-critical transition in double quantum dots

Luis G. G. V. Dias da Silva,<sup>1,\*</sup> Nancy P. Sandler,<sup>1</sup> Kevin Ingersent,<sup>2</sup> and Sergio E. Ulloa<sup>1</sup>

<sup>1</sup>*Department of Physics and Astronomy, Nanoscale and Quantum Phenomena Institute, Ohio University, Athens, Ohio 45701-2979*

<sup>2</sup>*Department of Physics, University of Florida, P.O. Box 118440, Gainesville, Florida, 32611-8440*  
(Dated: June 4, 2021)

Double quantum dots offer unique possibilities for the study of many-body correlations. A system containing one Kondo dot and one effectively noninteracting dot maps onto a single-impurity Anderson model with a structured (nonconstant) density of states. Numerical renormalization-group calculations show that while band filtering through the resonant dot splits the Kondo resonance, the singlet ground state is robust. The system can also be continuously tuned to create a pseudogapped density of states and access a quantum critical point separating Kondo and non-Kondo phases.

PACS numbers: 72.15.Qm, 73.63.Kv, 73.23.-b

The Kondo effect, arising from antiferromagnetic correlations between an unpaired spin and an electron bath [1], can be strongly modified by structure in the host density of states (DoS). Geometric confinement [2] and narrow bands [3] can dramatically change the Kondo state, with important observable consequences [4]. In pseudogapped hosts, where the DoS vanishes as a power-law at the Fermi energy, a quantum critical point (QCP) separates the Kondo phase from one at smaller couplings in which the Kondo effect is completely suppressed [5, 6, 7].

Semiconductor quantum dots provide many opportunities for systematic investigation of strong-correlation effects [8]. Single quantum dots have allowed controlled realizations of the Kondo regime of the Anderson impurity problem [9]. Recent attention has focused on the fascinating physics promised by double quantum-dot (DQD) systems [10]. For example, DQD experiments have investigated the effect of interdot “hybridization” on Kondo physics [11], and have beautifully demonstrated the competition between the Kondo effect and the Ruderman-Kittel-Kasuya-Yosida interaction among localized spins [12]. DQD setups have also been proposed to realize the unusual non-Fermi-liquid properties associated with the two-channel Kondo effect [13].

In this paper, we propose DQDs as a versatile experimental realization of an impurity coupled to an electron bath having a structured (nonconstant) DoS. Devices with one dot (“dot 1”) in the Kondo regime and the other (“dot 2”) close to resonance with the leads can be designed to produce an effective DoS having sharp resonances and/or pseudogaps near the Fermi energy. These features are shown to strongly modify the Kondo state, resulting in a wide range of DQD behavior, which we explore using numerical renormalization-group methods.

We show that when dot 1 is coupled to the leads *only through* dot 2, the Kondo resonance on dot 1 develops a sizable splitting. Unlike magnetic fields, which produce similar splittings, the “band filtering” introduced by the connecting dot preserves the Kondo singlet ground state, and results in a finite Kondo temperature for complete

screening of the magnetic moment on dot 1.

A second configuration, involving coherent dot-dot coupling via the leads, can mimic an Anderson impurity in a pseudogapped host. The device can be tuned by varying gate voltages to a QCP separating Kondo-screened and free-local-moment ground states. Such DQDs offer an attractive experimental setting for systematic study of boundary quantum phase transitions.

The DQD consists of dots 1 and 2 connected to left ( $L$ ) and right ( $R$ ) leads as well as to each other, as shown schematically in Fig. 1. We focus on situations in which dot 1 is tuned to have an odd number of electrons in a Coulomb blockade valley, so that it has an unpaired spin, while near-resonant transport through dot 2 is dominated by a single level [14] having a dot-lead coupling greater than the charging energy, so that the dot can be considered noninteracting. Our Hamiltonian is therefore

$$H = \sum_{i,\sigma} \varepsilon_i n_{i\sigma} + U_1 n_{1\uparrow} n_{1\downarrow} + \sum_{\sigma} \left( \lambda a_{1\sigma}^{\dagger} a_{2\sigma} + \text{H.c.} \right) + \sum_{j,\mathbf{k},\sigma} \varepsilon_{\mathbf{k}} c_{j\mathbf{k}\sigma}^{\dagger} c_{j\mathbf{k}\sigma} + \sum_{i,j,\mathbf{k},\sigma} \left( V_{ij} a_{i\sigma}^{\dagger} c_{j\mathbf{k}\sigma} + \text{H.c.} \right), \quad (1)$$

where  $a_{i\sigma}^{\dagger}$  creates a spin- $\sigma$  electron in dot  $i$  ( $= 1, 2$ ),  $n_{i\sigma} = a_{i\sigma}^{\dagger} a_{i\sigma}$ , and  $c_{j\mathbf{k}\sigma}^{\dagger}$  creates a spin- $\sigma$  electron of wavevector  $\mathbf{k}$  and energy  $\varepsilon_{\mathbf{k}}$  in lead  $j$  ( $= L, R$ ). For simplicity, we take the dot-lead couplings  $V_{ij}$  to be  $\mathbf{k}$ -independent. We further assume  $V_{iR} = V_{iL}$ , in which case the dots couple to the leads only in the symmetric combination  $c_{\mathbf{k}\sigma} = (c_{L\mathbf{k}\sigma} + c_{R\mathbf{k}\sigma})/\sqrt{2}$  and Eq. (1) describes double dots effectively coupled to a *single* lead, with  $V_i \equiv \sqrt{2}V_{iL}$ . Near-symmetric couplings can be achieved experimentally by appropriate tuning of the dot-lead tunneling gate voltages (see, e.g., [11]).  $V_i$  and the dot-dot coupling  $\lambda$  are taken to be real and positive.

The Green’s function (GF) for dot 1 is  $G_{11}(\omega) \equiv \langle\langle a_{1\sigma} : a_{1\sigma}^{\dagger} \rangle\rangle = (1 + U_1 \Gamma_{11}(\omega)) G_{11}^{(0)}(\omega)$ , where  $\omega$  is the energy relative to the common chemical potential  $\mu = 0$  in the leads,  $\Gamma_{11}(\omega) = \langle\langle n_{1,-\sigma} a_{1\sigma} : a_{1\sigma}^{\dagger} \rangle\rangle$ , and  $G_{11}^{(0)}(\omega)$  is the

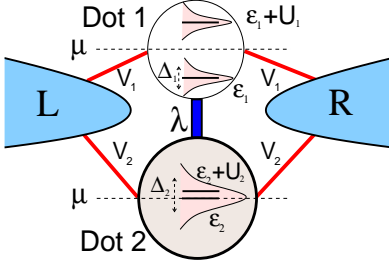


FIG. 1: (color online) Schematic of the DQD system. Dot 1 is Kondo-like ( $-\varepsilon_1, \varepsilon_1 + U_1 \gg \Delta_1 = \pi\rho_0 V_1^2$ , where  $\rho_0$  is the lead DoS), while dot 2 can be treated as a single, noninteracting ( $U_2 \ll \Delta_2 = \pi\rho_0 V_2^2$ ) resonant level.

noninteracting GF for dot 1 in the presence of dot 2:

$$\begin{aligned} [G_{11}^{(0)}(\omega)]^{-1} &= [G_1^{(0)}(\omega)]^{-1} - G_2^{(0)}(\omega) \times \\ &\left[ \lambda^2 + \lambda \sum_{\mathbf{k}} \frac{2V_1 V_2}{(\omega - \varepsilon_{\mathbf{k}})} + \sum_{\mathbf{k}, \mathbf{k}'} \frac{V_1^2 V_2^2}{(\omega - \varepsilon_{\mathbf{k}})(\omega - \varepsilon_{\mathbf{k}'})} \right], \quad (2) \end{aligned}$$

$G_i^{(0)}(\omega) = [\omega - \varepsilon_i - \sum_{\mathbf{k}} V_i^2 / (\omega - \varepsilon_{\mathbf{k}})]^{-1}$  being the noninteracting GF for dot  $i$  in the absence of the other dot.

Hereafter, we assume a constant DoS  $\rho_0$  in the leads. In the wide-band limit (half bandwidth  $D \gg |\omega|$ ), we can formally write  $[G_{11}(\omega)]^{-1} = \omega - \varepsilon_1 - \Sigma_{11}^*(\omega) + \Lambda(\omega) + i\Delta(\omega)$ , where  $\Sigma_{11}^*(\omega)$  is the proper self-energy,  $\Lambda(\omega) = \pi\rho_2(\omega) [(\lambda^2 - \Delta_1\Delta_2)(\omega - \varepsilon_2)/\Delta_2 - 2\lambda\sqrt{\Delta_1\Delta_2}]$ , and

$$\Delta(\omega) = \pi\rho_2(\omega) \left[ \lambda + (\omega - \varepsilon_2)\sqrt{\Delta_1/\Delta_2} \right]^2, \quad (3)$$

with  $\Delta_i = \pi\rho_0 V_i^2$  and  $\rho_2(\omega) = \Delta_2 / \{\pi[(\omega - \varepsilon_2)^2 + \Delta_2^2]\}$ .

All information on the coupling of dot 1 to the leads and to dot 2 enters  $G_{11}$  through  $\Lambda(\omega)$  (which essentially renormalizes the single-particle energy  $\varepsilon_1$ ) and, more importantly, through  $\Delta(\omega)$ . This provides a mapping of the DQD onto a single Anderson impurity coupled to a Fermi system with an *effective hybridization function*  $\Delta(\omega)$ , which “filters” the band states seen by dot 1 and modifies its coupling to the leads. We have solved this interacting model using an extension of the numerical renormalization-group (NRG) method [15] designed to handle arbitrary conduction band shapes [6].

In order to understand the effects of the *nonconstant* effective hybridization  $\Delta(\omega)$ , we consider (i) a *side-dot* configuration, in which dot 1 is coupled to the leads only through dot 2 ( $\lambda \neq 0, V_1 = 0$ ); (ii) a *parallel* configuration, in which interdot interactions take place only indirectly via the leads ( $\lambda = 0, V_1 \neq 0$ ); and (iii) a more general *fully connected* configuration ( $\lambda \neq 0, V_1 \neq 0$ ).

(i) In the *side-dot configuration*, the effective hybridization  $\Delta(\omega) = \pi\rho_2(\omega)\lambda^2$ , so the system maps onto an Anderson impurity coupled to a Lorentzian DoS. The case  $\varepsilon_2 = 0$ , which places the peak in  $\Delta(\omega)$  at the Fermi energy  $\omega = 0$ , yields the most striking properties.

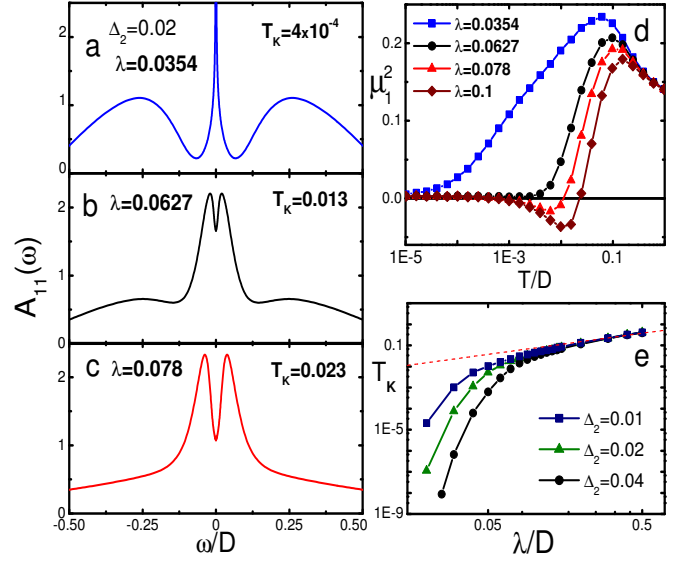


FIG. 2: (color online) Side-dot configuration. (a)–(c) Dot-1 spectral density for  $U_1 = -2\varepsilon_1 = 0.5$ ,  $\varepsilon_2 = 0$ , and  $\Delta_2 = 0.02$ . Splitting appears in  $A_{11}(\omega)$  for larger  $\lambda$  such that  $T_K \gtrsim \Delta_2/\sqrt{2}$ . (d) Effective moment  $\mu_1^2$  vs  $T$ . (e)  $T_K$  vs  $\lambda$ . For large  $\lambda$ ,  $T_K \propto \lambda$  (dashed). (Energies and  $T_K$  in units of  $D$ .)

Figure 2 presents results for  $\varepsilon_2 = 0$  and  $U_1 = -2\varepsilon_1$ , for which parameters the model exhibits strict particle-hole symmetry. Figs. 2(a)–(c) show the spectral density  $A_{11}(\omega) = -\text{Im} G_{11}(\omega)/\pi$  for  $\Delta_2 = 0.02D$  and different interdot couplings  $\lambda$ . For small  $\lambda$  [Fig. 2(a)], the spectral density resembles that for a constant DoS, its main features being broad Hubbard bands centered near  $\omega = \varepsilon_1$  and  $\varepsilon_1 + U_1$ , and a sharp resonance at  $\omega = 0$  having a width of order the Kondo temperature  $T_K$  (defined below). In this regime, the nonconstant  $\Delta(\omega)$  manifests itself through a generalized Fermi-liquid relation [16]  $A_{11}(0) = \cos^2 \varphi / [\pi\Delta(0)]$ , where  $\varphi = \int_{-\infty}^0 [(d\Delta/d\omega)\text{Re} G_{11}(\omega) - (d\Lambda/d\omega)\text{Im} G_{11}(\omega)] d\omega$ , i.e.,  $A_{11}(0)$  is smaller by a factor of  $\cos^2 \varphi$  than the standard result [1] for a flat band with the same  $\Delta(0)$ .

For larger  $\lambda$ , such that  $T_K \gtrsim \Delta_2/\sqrt{2}$ , the spectral density is qualitatively different. The Kondo resonance initially rises under the influence of the relatively weak hybridization found for  $|\omega| \gtrsim T_K$ . However, the upturn in  $\Delta(\omega)$  at  $|\omega| \lesssim \Delta_2$  causes  $A_{11}(\omega)$  to drop to satisfy  $A_{11}(0) \leq 1/[\pi\Delta(0)]$  (see above), splitting the resonance into two distinct peaks [Fig. 2(b)]. As  $\lambda$  increases further, the dip deepens and the Kondo peaks move out, eventually subsuming the Hubbard bands [Fig. 2(c)].

The splitting of the Kondo peak and the suppression of  $A_{11}(0)$  might be supposed to signal the destruction of the Kondo singlet ground state (as is the case in a magnetic field). However, this interpretation is refuted by the NRG many-body spectra, which show that the Kondo ground state is reached even for  $T_K \gg \Delta_2$ .

The progressive screening of the localized spin with

decreasing temperature  $T$  can be seen Fig. 2(d), which plots the square of the effective free moment on dot 1,  $\mu_1^2(T) \equiv T\chi_{\text{imp}}$ , where  $\chi_{\text{imp}}$  is the dot contribution to the zero-field susceptibility. The behavior for  $T_K \lesssim \Delta_2$  follows that for a constant DoS [15], crossing at  $T \approx |\varepsilon_1|$  from the free-orbital regime ( $\mu_1^2 \approx 1/8$ ) to the local-moment (LM) regime ( $\mu_1^2 \approx 1/4$ ), and then for  $T \ll T_K$ , to the strong-coupling (SC) Kondo limit in which the magnetic moment is totally screened ( $\mu_1 = 0$ ).

For  $T_K \gtrsim \Delta_2$ , the system still reaches the Kondo fixed point with  $\mu_1^2 = 0$  as  $T \rightarrow 0$ . However, the dot spin now exhibits an interesting window of *diamagnetic* behavior ( $\chi_{\text{imp}} < 0$ ), which becomes more pronounced as  $T_K$  increases [Fig. 2(d)]. This diamagnetic region arises from a negative term  $\propto d\rho_2(\omega)/d\omega$  in  $\chi_{\text{imp}}$  [16].

Since  $\mu_1^2$  in all cases passes from  $1/8$  at high temperatures to 0 at  $T = 0$ , we define the Kondo temperature using the standard criterion  $\mu_1^2(T_K) = 0.0701$  [15].  $T_K$ , shown in Fig. 2(e) for three different  $\Delta_2$  values, increases rapidly for small  $\lambda$ , and satisfies  $T_K \propto \lambda$  in the noninteracting narrow-band limit  $\lambda \gg \Delta_2, U_1/2$ .

The splitting observed in the Kondo resonance and the diamagnetic region in  $\mu_1^2(T)$  are produced by the sharp peak in  $\rho_2(\omega)$  at  $\omega = 0$  resulting from the resonance in dot 2. The resonance acts as a *filter* for the higher-energy states in the leads, reducing the effective conduction bandwidth connected to dot 1. This interpretation, which is consistent with similar findings of a negative  $\chi_{\text{imp}}$  in narrow-band systems [3], clearly differentiates the side-dot behavior from the peak splittings due to coherent coupling to a second Anderson impurity and the resulting suppression of the singlet state [11].

The side-dot behavior can also be understood as arising from *interference* between resonances. This can be seen by considering the noninteracting spectral density  $A_{11}^{(0)} = -\text{Im} G_{11}^{(0)}/\pi$  for  $\varepsilon_1 = \varepsilon_2$ . For  $\lambda < \Delta_2/\sqrt{2}$ ,  $A_{11}^{(0)}$  has a single peak (width  $\sim \lambda^2$ ) at  $\omega = \varepsilon_2$ ; whereas for  $\lambda > \Delta_2/\sqrt{2}$ , there are two peaks at  $\omega = \varepsilon_2 \pm \sqrt{\lambda^2 - \Delta_2^2/2}$ , arising from interference between the  $\omega = 0$  single-particle resonances on the two dots. The NRG results for the interacting case are closely analogous: For  $T_K \lesssim \Delta_2/\sqrt{2}$ ,  $A_{11}$  has a single peak (width  $\sim T_K$ ) at  $\omega = \varepsilon_2 = 0$ , while for  $T_K \gtrsim \Delta_2/\sqrt{2}$ , there are two peaks, in this case resulting from interference between the  $\omega = 0$  many-body Kondo resonance and the  $\omega = 0$  single-particle resonance in  $\rho_2$ . The separation of the peaks in  $A_{11}$  increases with  $T_K - \Delta_2$ , further supporting the analogy.

(ii) The *parallel configuration* ( $\lambda = 0$ ) exhibits very different behavior. For  $\varepsilon_2 = 0$ , the hybridization  $\Delta(\omega)$  [Eq. (3)] *vanishes* at  $\omega = 0$  as  $|\omega|^r$  with  $r = 2$  [see Fig. 3(a)], and the DQD setup maps onto an Anderson impurity in a pseudogapped host [17]. The properties of such system depend strongly on the exponent  $r$  and on the presence or absence of  $p$ - $h$  symmetry [6, 7]. For  $r = 2$ , the SC phase is inaccessible at  $p$ - $h$  symmetry, but away from

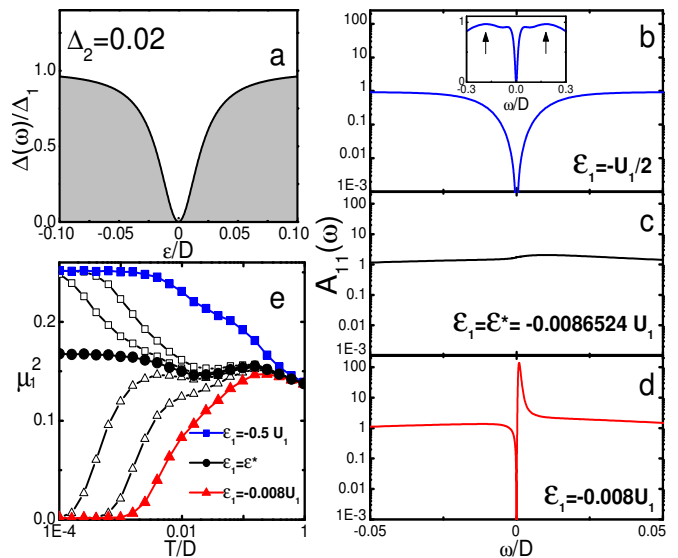


FIG. 3: (color online) Parallel DQD with  $U_1 = 0.5$ ,  $\Delta_1 = 0.05$ ,  $\Delta_2 = 0.02$ , and  $\varepsilon_2 = 0$ . (a) Hybridization  $\Delta(\omega)$  vanishes as  $|\omega|^2$  at  $\omega = 0$ . (b)–(d) Dot-1 spectral density  $A_{11}(\omega)$ , and (e) effective moment  $\mu_1^2(T)$ , for various  $\varepsilon_1$ . For  $\varepsilon_1 \approx -U_1/2$ , no Kondo effect occurs:  $A_{11}(0) = 0$  in (b), and  $\mu_1^2(0) = 1/4$  [■ and □ in (e)]. This LM phase is separated by a QCP at  $\varepsilon_1 = \varepsilon^* > -U_1/2$ , characterized by a featureless  $A_{11}(\omega)$  in (c) and  $\mu_1^2(0) = 1/6$  [● in (e)], from the SC phase [(d), ▲ and △ in (e)] in which  $A_{11}$  vanishes at  $\omega = 0$  and peaks at some  $\omega > 0$ .

this special limit, a QCP separates SC and LM phases.

In the  $p$ - $h$ -symmetric case  $\varepsilon_1 = -U_1/2$ , the Kondo resonance in  $A_{11}$  disappears completely [Fig. 3(b)], but Hubbard bands are still present (arrows in inset).  $A_{11}$  vanishes at  $\omega = 0$  as  $\omega^2$ , and  $\mu_1^2(0) = 1/4$  [Fig. 3(e)], as expected in the LM phase [6] where no Kondo effect occurs. When  $p$ - $h$  symmetry is broken by increasing  $\varepsilon_1$ , the same qualitative behavior persists [squares in Fig. 3(e)] until the QCP is reached at  $\varepsilon_1 = \varepsilon^*$ , where  $A_{11}$  is nearly featureless [Fig. 3(c)] and  $\mu_1^2(0) = 1/6$  [circles in Fig. 3(e)]. For  $\varepsilon_1 > \varepsilon^*$ , the system enters the SC phase in which  $\mu_1^2(0) = 0$  [triangles in Fig. 3(e)], indicating complete Kondo screening of dot 1, and  $A_{11}$  again goes to zero as  $\omega^2$  at  $\omega = 0$ , but (in contrast to the LM phase), there is a distinct peak at positive  $\omega$  [Fig. 3(d)].

(iii) In the *fully connected configuration* ( $V_1, V_2$ , and  $\lambda$  all nonzero),  $\Delta(\omega)$  has an asymmetric Fano-like shape, peaking at  $\varepsilon_2 + \sqrt{\Delta_1 \Delta_2^3}/\lambda$ , and vanishing as  $(\omega - \omega_0)^2$  at  $\omega_0 = \varepsilon_2 - \lambda\sqrt{\Delta_2/\Delta_1}$ . Here, the DQD properties can be controlled not only by tuning  $\lambda$ ,  $\Delta_1$ , or  $\Delta_2$  [as in (i) and (ii)], but also by using external gate voltages to vary  $\varepsilon_2$ .

Figures 4(a)–(e) show the evolution of  $\Delta(\omega)$  as  $\varepsilon_2$  shifts across the Fermi energy. Generically, the dot-1 spectral density features a  $p$ - $h$ -asymmetric Kondo resonance, whose width  $T_K$  is primarily determined by  $\Delta(0)$  [Figs. 4(f), (h), (j)]. However, when the peak of  $\Delta(\omega)$  approaches  $\omega = 0$ ,  $T_K$  is enhanced and the Kondo peak splits [Fig. 4(g)]. By contrast, when the zero of  $\Delta(\omega)$  approaches

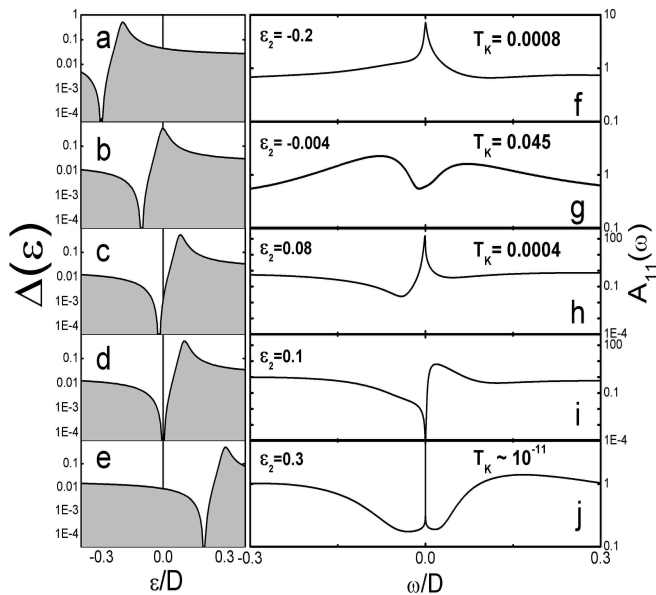


FIG. 4: Fully connected DQD with  $U_1 = -2\varepsilon_1 = 0.5$ ,  $\Delta_1 = \Delta_2 = 0.02$ , and  $\lambda = 0.1$ . (a)–(e) Hybridization  $\Delta(\omega)$  for various  $\varepsilon_2$ , and (f)–(j) the corresponding  $A_{11}(\omega)$ . An asymmetric Kondo peak appears when  $\Delta(\omega)$  is featureless near  $\omega = 0$  (a, e). The peak splits as the resonance in  $\Delta(\omega)$  approaches  $\omega = 0$  (b), reappears in the intermediate region (c), and disappears altogether when a pseudogap forms (d).

the Fermi energy, the Kondo temperature decreases, and if  $\omega_0$  is tuned to zero, pseudogap behavior is recovered with complete suppression of the Kondo peak [Fig. 4(i)].

In summary, we have shown that double quantum-dot (DQD) systems with one of the dots in the Kondo regime can be tailored experimentally to explore the effects of a nonconstant density of states (DoS) on the many-body ground-state properties. In setups where the Kondo dot is decoupled from the reservoirs, the Kondo resonance on that dot undergoes zero-field splitting for large interdot coupling. This can be understood as the coherent interaction between the many-body Kondo state and a single-particle resonance in the second dot. Although the Kondo peak in the spectral density at the Fermi energy is suppressed, the Kondo singlet state is robust, and the localized spin is completely screened at low temperatures. In this regime, the system also passes through a temperature window of diamagnetic behavior, similar to that seen in narrow-band systems.

For weak interdot couplings, the Kondo state is suppressed by the presence of a pseudogap in the effective DoS, and a quantum phase transition takes place between local-moment and Kondo-screened phases. A quantum critical point on the boundary between these phases can be reached by appropriate tuning of the experimental parameters. Thus, DQD systems provide a rare example of a controlled setting in which to investigate quantum critical behavior in a strongly correlated system.

This work was partially supported by NSF DMR–

0312939 (K.I.) and NSF-IMC/NIRT (L.D.S., N.S., S.U.).

\* Electronic address: dias@phy.ohiou.edu

- [1] A. C. Hewson, *The Kondo Problem to Heavy Fermions* (Cambridge Univ. Press, Cambridge, England, 1997).
- [2] W. B. Thimm, J. Kroha, and J. von Delft, *Phys. Rev. Lett.* **82**, 2143 (1999); P. S. Cornaglia and C. A. Balseiro, *Phys. Rev. B* **66**, 174404 (2002); P. Simon and I. Affleck, *Phys. Rev. Lett.* **89**, 206602 (2002); P. S. Cornaglia and C. A. Balseiro, *ibid.* **90**, 216801 (2003); C. H. Booth *et al.*, *ibid.* **95**, 267202 (2005); R. K. Kaul *et al.*, cond-mat/0601274 (2006).
- [3] W. Hofstetter and S. Kehrein, *Phys. Rev. B* **59**, R12732 (1999).
- [4] A. A. Aligia and A. M. Lobos, *J. Phys. Condens. Matter* **17**, S1095 (2005).
- [5] D. Withoff and E. Fradkin, *Phys. Rev. Lett.* **64**, 1835 (1990); K. Chen and C. Jayaprakash, *J. Phys. Condens. Matter* **52**, 14436 (1995); K. Ingersent, *Phys. Rev. B* **54**, 11936 (1996).
- [6] R. Bulla, T. Pruschke, and A. C. Hewson, *J. Phys. Condens. Matter* **9**, 10463 (1997); C. Gonzalez-Buxton and K. Ingersent, *Phys. Rev. B* **57**, 14254 (1998).
- [7] L. Fritz and M. Vojta, *Phys. Rev. B* **70**, 214427 (2004).
- [8] L. Sohn, L. Kowenhoven, and G. Schön, *Mesoscopic Electron Transport* (Kluwer, New York, 1997).
- [9] D. Goldhaber-Gordon *et al.*, *Nature* **391**, 156 (1998); S. M. Cronenwett, T. H. Oosterkamp, and L. P. Kouwenhoven, *Science* **281**, 540 (1998).
- [10] B. A. Jones, C. M. Varma, and J. W. Wilkins, *Phys. Rev. Lett.* **61**, 125 (1988); R. Aguado and D. C. Langreth, *ibid.* **85**, 1946 (2000); M. R. Li and K. Le Hur, *ibid.* **93**, 176802 (2004); G. B. Martins *et al.*, *ibid.* **94**, 026804 (2005); P. Simon, R. Lopez, and Y. Oreg, *ibid.* **94**, 086602 (2005); M. R. Galpin, D. E. Logan, and H. R. Krishnamurthy, *ibid.* **94**, 186406 (2005); R. Lopez *et al.*, *Phys. Rev. B* **71**, 115312 (2005).
- [11] H. Jeong, A. M. Chang, and M. R. Melloch, *Science* **293**, 2221 (2001); J. C. Chen, A. M. Chang, and M. R. Melloch, *Phys. Rev. Lett.* **92**, 176801 (2004).
- [12] N. J. Craig *et al.*, *Science* **304**, 565 (2004).
- [13] Y. Oreg and D. Goldhaber-Gordon, *Phys. Rev. Lett.* **90**, 136602 (2003); M. Pustilnik, L. Borda, L. I. Glazman, and J. von Delft, *Phys. Rev. B* **69**, 115316 (2004).
- [14] This condition on dot 2 might be satisfied by (i) a large, chaotic dot which level-broadening fluctuations cause transport to be dominated by a few strongly coupled levels [P. G. Silvestrov and Y. Imry, *Phys. Rev. Lett.* **85**, 2565 (2000)] or (ii) a small dot, in which the mean level spacing exceeds the charging energy, as recently realized in nanowire-embedded dots [M. T. Bjork *et al.*, *Nano Lett.* **4**, 1621 (2004)].
- [15] H. R. Krishnamurthy, J. W. Wilkins, and K. G. Wilson, *Phys. Rev. B* **21**, 1003 (1980). In that paper's notation, we have set  $\Lambda = 2.5$  and kept 800–1200 ( $Q, S$ ) states.
- [16] L. G. G. V. Dias da Silva, N. P. Sandler, K. Ingersent, and S. E. Ulloa (in preparation).
- [17] This mapping holds even for  $V_{iR} \neq V_{iL}$  provided that  $V_{iL}V_{2R} = V_{iR}V_{2L}$ ; otherwise,  $\Delta(0)$  is small but nonzero.